ORIGINAL RESEARCH

Identification and Validation of Hub Immune-Related Genes in Non-Alcoholic Fatty Liver Disease

Juyi Li[1,2], Chunjia Kou[1], Tiantian Sun[3], Jia Liu[3–5], Haiqing Zhang[1,3–5]

[1]Department of Endocrinology, Shandong Provincial Hospital, Shandong University, Jinan, Shandong, 250021, People's Republic of China; [2]Department of Endocrinology, Geriatrics Center, The First Affiliated Hospital of Anhui University of Chinese Medicine, Hefei, Anhui, 230001, People's Republic of China; [3]Department of Endocrinology, Shandong Provincial Hospital Affiliated to Shandong First Medical University, Jinan, Shandong, 250021, People's Republic of China; [4]Shandong Clinical Medical Center of Endocrinology and Metabolism, Jinan, Shandong, People's Republic of China; [5]Institute of Endocrinology and Metabolism, Shandong Academy of Clinical Medicine, Jinan, Shandong, People's Republic of China

Correspondence: Jia Liu, No. 324, Five-Jing Road, Jinan, Shandong Province, China, Email liujia_625@163.com; Haiqing Zhang, No. 324, Five-Jing Road, Jinan, Shandong Province, China, Email haiqingzhang7576@163.com

Background: Nonalcoholic fatty liver disease (NAFLD) is the most common progressive liver disease worldwide. It can cause liver cancer and possibly death. Abnormal immune infiltration is involved in the progression of NAFLD. The aim of this study was to identify and validate the hub immune-related genes in NAFLD.

Methods: Microarray data were downloaded from Gene Expression Omnibus, and immune-related differentially expressed genes (IRDEGs) were obtained. A protein–protein interaction network was used to further screen. The diagnostic value of the IRDEGs was evaluated by receiver operating characteristic curves. Differences in immune infiltration levels were analyzed using single-sample gene set enrichment analysis. Hub IRDEGs were identified by correlation analysis with immune infiltration levels. Finally, molecular experiments were used to confirm the expression of the hub IRDEGs and explore their roles in NAFLD.

Results: We obtained 18 IRDEGs. Five hub genes were further identified by protein–protein interaction network, receiver operating characteristic curves and correlation analysis: AQP9, BACH2, CD4, IL17RE and S100A9. Based on functional enrichment analysis, the hub genes were enriched primarily in many immune-related pathways. In NAFLD, AQP9, CD4, and IL17RE expression was significantly reduced, whereas BACH2 and S100A9 expression was elevated. PCR, oil red O staining and triglyceride detection revealed that the knock-down of BACH2 and S100A9 reduced lipid accumulation in NAFLD cells.

Conclusion: This study provided insight into the profile of immune infiltration underlying NAFLD and identified AQP9, BACH2, CD4, IL17RE and S100A9 as ancillary diagnostic indicators of NAFLD. And BACH2 and S100A9 might be therapeutic targets for NAFLD.

Keywords: nonalcoholic fatty liver disease, immune infiltration, BTB domain and CNC homolog 2, BACH2, S100 calcium binding protein A9, S100A9

Introduction

Nonalcoholic fatty liver disease (NAFLD) is a potentially serious liver disease. 2019 data suggested that the prevalence of NAFLD in Asia had exceeded 30%, as high as the figures for Europe and North America.[1–3] NAFLD is characterized by liver steatosis without a clear cause such as excessive alcohol consumption.[4] Liver steatosis alone has a 20–30% chance of progressing to nonalcoholic steatohepatitis (NASH). And NASH may lead to cirrhosis, liver failure, and even hepatocellular carcinoma (HCC).[5,6] Notably, even in the absence of cirrhosis, NAFLD may predispose patients to HCC.[7] Therefore, NAFLD is currently a widespread public health issue.

Abnormal lipid accumulation has been demonstrated to cause liver inflammation, a hallmark of NAFLD progression to HCC.[8] During this process, the immune system is abnormally activated, resulting in harmful inflammation. This state could lead to increased liver infiltration and the accumulation of inflammatory cells, which exacerbates liver damage.[9] Furthermore, NAFLD can promote HCC development by inducing apoptosis in CD4+ T cells.[10] Therefore, identifying the immune-related molecular mechanisms that play a role in the progression of NAFLD is critical for both early diagnosis and the discovery of new treatment targets.

The advancement of bioinformatics has made it possible to address the aforementioned questions. To date, various methods, such as functional enrichment analysis and immune infiltration analysis, have been widely used to investigate the molecular mechanisms of disease development. The aim of this study was to search for hub immune-related genes in the development of NAFLD by a series of bioinformatics analyses. Next, we explored the role of hub genes in NALFD. In addition, we calculated the diagnostic value of the hub genes to aid in clinical diagnosis. Finally, we performed molecular experiments to validate our findings.

Methods and Materials

Data Collection and Processing

Microarray expression data for NAFLD were downloaded from Gene Expression Omnibus. The GSE160016 dataset included data for 5 patients with NAFLD and 6 healthy controls.[11] When multiple probes were mapped to the same gene symbol, the mean value was selected as the gene expression value.

Identification of Immune-Related Differentially Expressed Genes (IRDEGs)

Differentially expressed genes (DEGs) were obtained using the limma package[12] with screening criteria of $P < 0.05$ and $|\log$ fold change (FC)$| > 1$. We obtained immune-related genes from the ImmPort database.[13] Marker genes for immune cells were obtained from a previous study.[14] DEGs that overlapped with both of these sets of genes were defined as IRDEGs.

Functional Analysis of IRDEGs

Gene Ontology (GO) and Kyoto Encyclopedia of Genes and Genomes (KEGG) enrichment analyses were used to understand the biological functions and signaling pathways of the IRDEGs associated with NAFLD. GO analysis included the categories of biological process (BP), cellular component (CC) and molecular function (MF). Disease Ontology (DO) enrichment analysis was used to identify diseases in which the IRDEGs might be involved. Finally, enrichment analysis of IRDEGs in tissues and cells was performed using the CellMarker database.[15]

To explore the potential mechanisms of immune function during NAFLD progression, the immunological signature gene set (c7.all.v7.5.1.symbols.gmt) in MSigDB was used as a reference for gene set enrichment analysis (GSEA). Genes for which $|$normalized enrichment score (NES)$| > 1$ and $P < 0.05$ were considered significantly enriched.

Finally, a protein–protein interaction (PPI) network for the IRDEGs was constructed using data from the STRING database with a confidence level of 0.4. Genes that did not interact with other nodes in this network were not included in further analyses. Furthermore, we used the maximal clique centrality (MCC) metric to determine the importance of individual nodes in the network.

Screening of Hub IRDEGs

With the data in GSE160016, we used receiver operating characteristic (ROC) curves to assess the diagnostic value for NAFLD of the IDEGs. Validation was performed using the GSE126848 dataset.

Single-sample gene set enrichment analysis (ssGSEA) was then used to investigate the level of immune infiltration in each sample. The resulting score was derived by calculating the expression levels of specific marker genes.[16] Box plots were used to show differences in immune infiltration levels. A gene that correlated with a differential immune infiltration level and had an area under the curve (AUC) greater than 0.7 in both datasets was defined as a hub IRDEG.

Functional Enrichment Analysis of Hub IRDEGs

Correlations between the expression of hub IRDEGs were calculated using Spearman correlation analysis. We used GeneMANIA to investigate the network of the hub IRDEGs and their coexpressed genes. Finally, GO and KEGG enrichment analyses were carried out to investigate the functions involving the hub IRDEGs.

Detecting the Role of Hub IRDEGs in NAFLD

Cell Culture, Animal Experiments and Clinical Samples

HepG2 cell line was purchased from Procell Biotechnology Co., Ltd. (Wuhan, China). The identification certificate of HepG2 was shown in Appendices I and II. Cells were maintained in MEM supplemented with 10% (v/v) heat-inactivated fetal bovine serum (FBS), penicillin G (100 units/mL) and streptomycin (100 μg/mL), and kept at 37°C in a humidified atmosphere containing 5% CO_2. Based on published literature, we used palmitic acid (PA) to establish a NAFLD cell model.[17,18] PA (Sigma, USA) was completely dissolved in anhydrous ethanol at a concentration of 500 mM and mixed with equimolar amounts of NaOH. This PA stock solution was added to the bovine serum albumin (BSA) solution to achieve a final PA concentration of 0.4 mmol/L, dissolved by heating in a water bath at 55 °C and filtered through a 0.22 um microporous membrane, and cooled to room temperature to obtain the PA-BSA complex which is the PA induction solution. Cells were inoculated in 6-well plates and then starved for 12 h. After that, PA induction solution was added and treated for 24 h.

The NAFLD model was established using C57BL/6 male mice according to previous studies.[19,20] In a short, regular diet was replaced with a diet containing 60 kcal% fat. In addition, the sex of the mice did not hinder the establishment of animal model. Mice were purchased from Vital River (Beijing, China). The livers from animals would be used for validation. National Institutes of Health guide for the care and use of Laboratory animals (NIH Publications No. 8023, revised 1978) had been followed.

Human blood samples were obtained from NAFLD patients at Shandong Provincial Hospital from November 2021 to November 2022. Inclusion criteria: (1) patients were diagnosed with NAFLD by ultrasonography and relevant blood biochemical tests, and met the relevant diagnostic criteria in the "Guidelines for the diagnosis and treatment of non-alcoholic fatty liver disease"[1] developed by the Chinese Medical Association, and had no history of excessive alcohol consumption (ethanol intake < 140g/week for men and < 70g/week for women); (2) patients had no abnormal mental status.

Exclusion criteria: (1) combined with other liver diseases such as viral hepatitis, immune hepatitis, alcoholic hepatitis; (2) combined with underlying diseases such as diabetes, hypertension, coronary artery disease or renal disease; (3) combined with autoimmune diseases or hematological diseases; (4) combined with malignant neoplasm; (5) received other medications within 4 weeks.

Healthy subjects who underwent physical examination at our hospital during the same period were selected as the controls. All vital signs were normal and there was no history of underlying diseases such as diabetes, hypertension and liver diseases. All patients and subjects had signed an informed consent form.

Cell Transfection

The small interference RNA (siRNA) of BACH2 and S100A9 and negative control siRNA (siNC) were purchased from Genechem (Shanghai, China). Cells were transfected according to the manufacturer's instructions. We used PCR to analyze transfection efficiency.

Quantitative Real-Time PCR and Immunohistochemistry

RNA was extracted using TRIzol reagent and PCR was performed to determine the mRNA expression levels of genes based on previous studies.[21] GAPDH was used as the internal control, and relative gene expression was calculated by the $2^{-\Delta\Delta Ct}$ method. The sequences of the primers used are listed in Supplemental Table 1.

Mice were anesthetized and sacrificed. The livers were made into deparaffinized sections. For immunohistochemistry analysis, we conducted it according to previous study.[22] The antibodies of BACH2 and S100A9 were purchased from Affinity Biosciences (Cincinnati, USA) and diluted according to the manufacturer's protocol. For all stains, samples with inadequate staining due to technical problems were excluded.

Oil Red O Staining and Triglyceride Detection

Based on published literature, we performed the oil red O staining to detect the lipid accumulation in cells.[23]

According to the manufacturer's instructions, we used commercially available kits (BC0625, Solarbio, China) to detect triglyceride in cells.

Statistical Analysis and Ethics Statements

All experiments were repeated at least three times independently. All statistical information was shown in the figures, figure legends. The data distribution was assumed to be normal but this was not formally tested. The allocation in animal experiments was random. Data collection and analysis were not blind to the conditions of the experiments. Continuous variables were expressed as the means ± standard deviations. The Student's *t*-test was used to determine the significance of differences. R (version 4.1.2) was used for all statistical analyses, and the significance level was set at P < 0.05. The codes used in this study were uploaded as Supplementary Materials.

The study was conducted according to the guidelines of the Declaration of Helsinki and approved by the Biomedical Research Ethic Committee of Shandong Provincial Hospital (SWYX: NO. 2021–270; SWYX: NO. 2021–497).

Results

Identification of IRDEGs

We identified 2033 DEGs based on the screening criteria: 833 upregulated genes and 1200 downregulated genes (Figure 1A). Eighteen IRDEGs were obtained after determining the overlap among the sets of genes (Figure 1B). The expression levels and $\log_2$FC values of these genes are shown in Figure 1C and D. More detailed data is shown in Table 1.

Functional Enrichment Analysis of the IRDEGs

KEGG signaling pathway enrichment analysis indicated that the IRDEGs were involved in various immune-related pathways, including antigen processing and delivery, the IL-17 signaling pathway, and the differentiation of Th1, Th2, and Th17 cells (Figure 2A). The IRDEGs were primarily enriched in BP terms related to defense processes (eg, defense responses against bacteria and fungi and cellular chemotaxis) (Figure 2B). In terms of CCs and MFs, the IRDEGs were closely related to MHC and fatty acid binding (Figure 2C and D). DO enrichment analysis revealed that the IRDEGs were also involved in numerous immune function-related diseases, such as psoriatic arthritis disorders (Figure 2E). As shown in Figure 2F, the IRDEGs were enriched primarily in T cells.

GSEA indicated that these gene sets were enriched primarily in CD4+ T cells and B cells. Figure 3 shows the top 15 enriched gene sets, and Supplemental Table 2 contains more information. In summary, these findings demonstrated that immune-related genes play a critical role in the development and progression of NAFLD.

Next, we used PPI analysis to perform a preliminary screen of the IRDEGs, yielding a network of 14 genes (Figure 4A). The MCC scores shown in Figure 4B revealed that the three most central genes in this network were CD4, S100A8, and S100A9.

Identification of Hub IRDEGs

To determine the diagnostic value of the IRDEGs in NAFLD, we first used GSE160016 as the training dataset. The findings revealed that most of the IRDEGs had a high diagnostic value (AUC > 0.7). Only nine genes (AQP9, BACH2, CCL20, CD4, GNLY, HLA-DPA1, HLA-DPB1, IL17RE, and S100A9) retained an AUC of greater than 0.7 after validation with GSE126848 (Figure 5).

We used ssGSEA with the GSE160016 dataset to analyze immune infiltration in NAFLD (Figure 6A). In Figure 6B, the Wilcoxon rank–sum test results revealed that the infiltration level of T helper cells, the infiltration level of Tfh cells, and the type I IFN response were decreased in NAFLD (P < 0.05). Next, we performed Spearman correlation analysis (Figure 6C and D). Finally, we identified five hub IRDEGs: AQP9, BACH2, CD4, IL17RE, and S100A9. The associations between the expression levels of these genes are shown in Figure 7A.

Functional Enrichment Analysis of the Hub IRDEGs

We further investigated the functions of the hub IRDEGs. As shown in Figure 7B and C, the hub genes were involved in various immune-related biological functions, such as immune receptor activity and inflammatory response regulation. These findings implied that the hub IRDEGs influence the progression of NAFLD by regulating immune function.
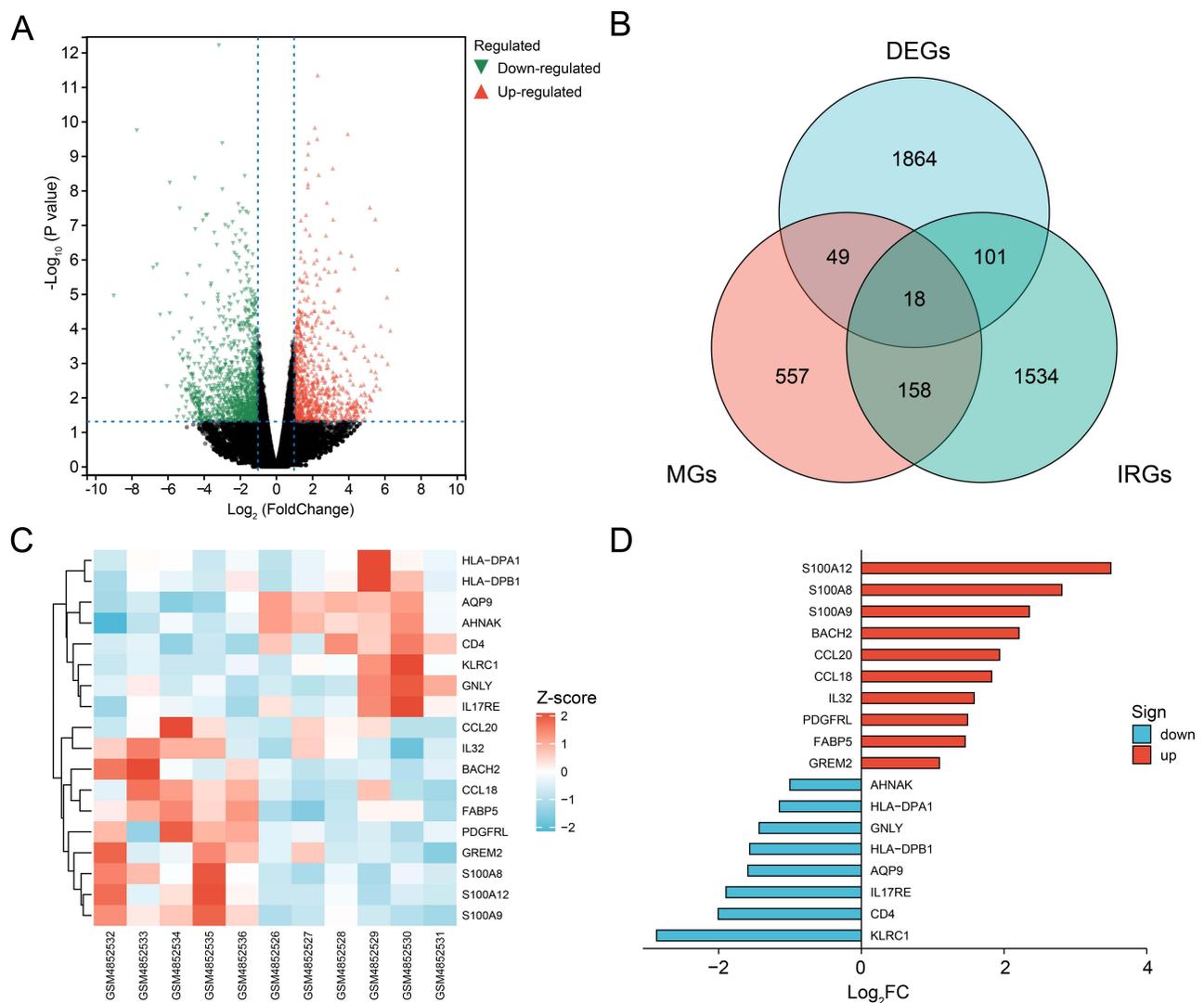
Figure 1 Identification of IRDEGs in NAFLD. Volcano map of DEGs (**A**). Venn diagram indicated the overlap of DEGs in NAFLD, immune-related genes from ImmPort database and marker genes of immune cells to obtain 18 IRDEGs (**B**). Heat plot and horizontal bar chart showed the expression profile and fold change of 18 IRDEGs (**C** and **D**).

Validation of Hub IRDEG Expression in NAFLD

We used quantitative real-time PCR to confirm the expression levels of the hub IRDEGs. As shown in Figure 7D, the expression of AQP9, CD4, and IL17RE was significantly lower but that of BACH2 and S100A9 was higher in NAFLD cells. The same trend was found for all genes except for IL17RE in the established NAFLD animal model (Figure 7E). Finally, we obtained blood samples from 18 NAFLD patients and 18 healthy controls. The expression levels of the hub IRDEGs in human blood were consistent with those in NAFLD cells (Figure 7F).

The Knock-Down of BACH2 and S100A9 Reduced Lipid Accumulation in NAFLD Cells

In five hub IRDEGs, the expression of BACH2 and S100A9 was up-regulated in NAFLD. Thus, we decided to explore their roles in NAFLD.

First of all, we further confirmed the histological expression of BACH2 and S100A9. As evidenced by immunohisto-chemical staining analysis, the expression of BACH2 and S100A9 was increased in the livers of NAFLD mice (Figure 8A).

Table 1 Detail Information of Eighteen IRDEGs

Gene Symbols	Log$_2$FC	P value	Regulated
S100A12	3.497	< 0.001	Up
S100A8	2.810	< 0.001	Up
S100A9	2.354	< 0.001	Up
BACH2	2.209	< 0.001	Up
CCL20	1.937	0.032	Up
CCL18	1.826	0.016	Up
IL32	1.581	0.001	Up
PDGFRL	1.489	0.033	Up
FABP5	1.455	0.001	Up
GREM2	1.094	0.004	Up
AHNAK	−1.002	0.001	Down
HLA-DPA1	−1.149	0.035	Down
GNLY	−1.433	0.044	Down
HLA-DPB1	−1.565	0.014	Down
AQP9	−1.591	< 0.001	Down
IL17RE	−1.896	0.003	Down
CD4	−2.007	< 0.001	Down
KLRC1	−2.870	0.012	Down

In Figure 8B, we successfully knocked down the expression of BACH2 and S100A9 in HepG2 cells. Next, we detected the expression of several marker genes of lipid accumulation (SREBP1c, FAS, SCD1 and ACC) (Figure 8C). We found that the expression of all marker genes decreased after transfection. In the NAFLD cell model established by PA, the same phenomenon was observed. Oil Red O staining revealed that siBAHC2 and siS100A9 inhibited the lipid accumulation and reduced triglyceride levels in NAFLD cells (Figure 8D and E).

Discussion

Recently, studies have confirmed that the immune system plays an important role in the initiation and progression of liver inflammation in patients with NAFLD.[9] Different T-cell populations are involved in the immunopathogenesis of NAFLD, and the progression from steatosis to NASH is accompanied by a progressive increase in the accumulation of natural killer T cells.[24] Since regulatory T cells and Th17 cells represent the two extremes of the immune response (tolerance and inflammation), it has been suggested that NAFLD progression may be associated with disruption of this balance.[25] Our data showed that the infiltration levels of helper T cells and Tfh cells were decreased in NAFLD, reflecting the diminished partial immune response in NAFLD. Moreover, a study by Ma et al demonstrated that NAFLD led to the loss of selective CD4+ T cells and promoted hepatocarcinogenesis.[10] These results suggest that the immune system is suppressed during hepatic progression from steatosis through NAFLD to HCC. However, data on the behavior of T cells in the liver are scarce, and we cannot yet identify the specific mechanisms that trigger this process. In addition, some studies have shown that adipose tissue may directly contribute to the progression of NAFLD through cytokines and immune signaling and lead to liver injury.[26,27]

In the present study, we identified five hub genes: AQP9, CD4, IL17RE, BACH2 and S100A9. Among these genes, AQP9 plays a major role in glycerol uptake by mouse hepatocytes.[28] One study reported that AQP9 expression was downregulated in a mouse model of NAFLD,[29] a pattern that was also found in the human liver.[30] However, some studies have shown that AQP9 overexpression increases the degree of steatosis.[31] These findings seem to be contradictory. We
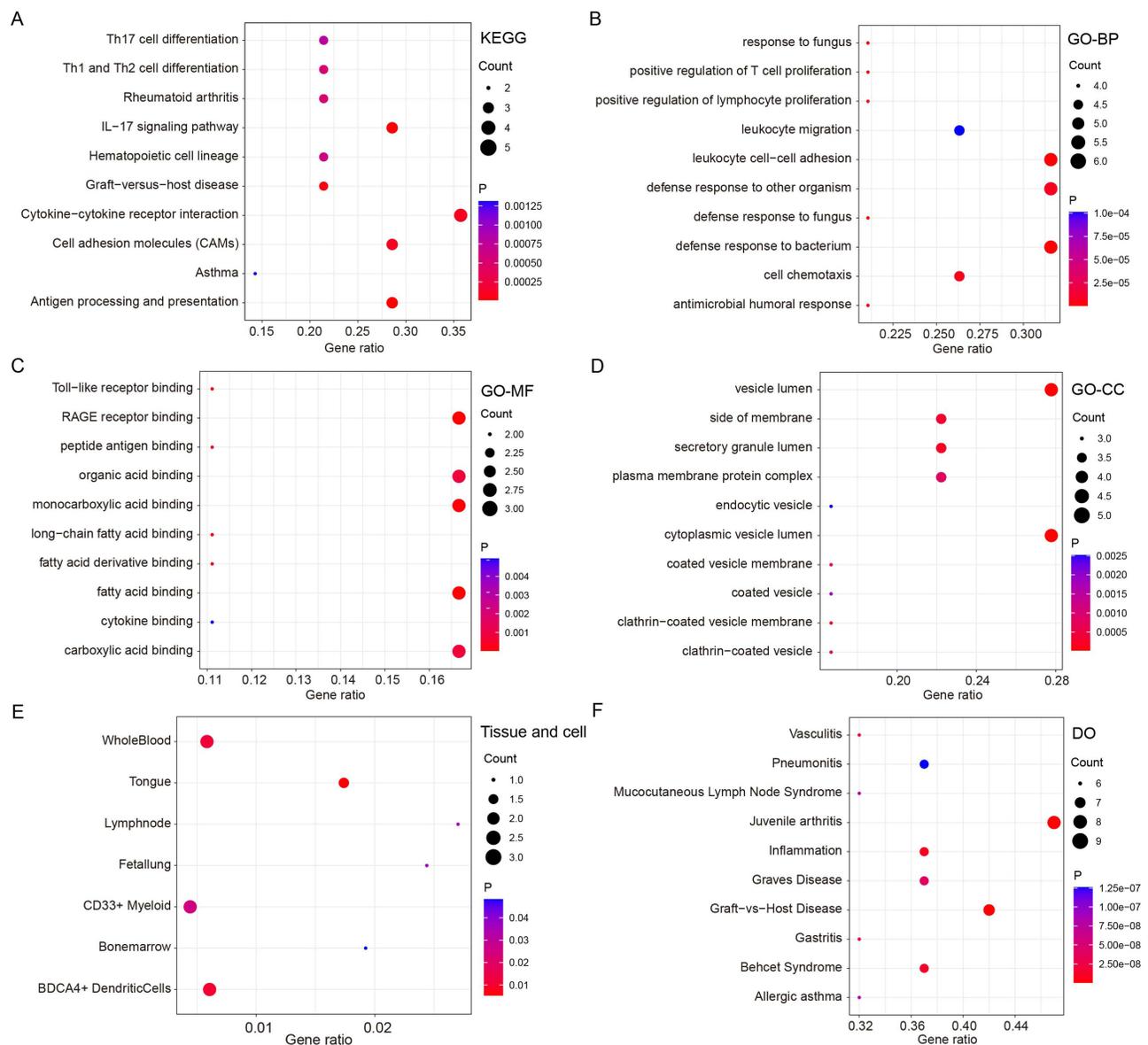
Figure 2 Functional enrichment analysis of IRDEGs. KEGG plot showed the top 10 enriched pathways of IRDEGs (**A**). GO plots showed the enriched functions of IRDEGs in biological processes (BP), cellular components (CC), and molecular functions (MF) (**B–D**). The enriched diseases, tissue and cell of IRDEGs (**E** and **F**).

think that the difference in the level of AQP9 expression may be due to the difference in the degree of steatosis, and further studies are needed to demonstrate this relationship.

S100A9 encodes a binding protein that plays an important role in the regulation of inflammatory processes and immune responses.[32–34] High expression levels of S100A9 have been identified in patients with cardiovascular disease and diabetes.[35,36] Our study showed upregulation of S100A9 expression in NAFLD. And siS100A9 could inhibited NAFLD progression. Consistent with previous studies, S100A9 had a high diagnostic value in NAFLD (AUC close to 1) and was a sensitive marker of NAFLD progression.[37] Thus, S100A9 undoubtedly has a high potential for clinical application.

Unlike the associations of the other three genes, the associations of IL17RE and BACH2 with NAFLD were previously identified. IL17RE acts as a receptor for interleukin-17C (IL-17C), and the IL-17C/IL17RE signaling
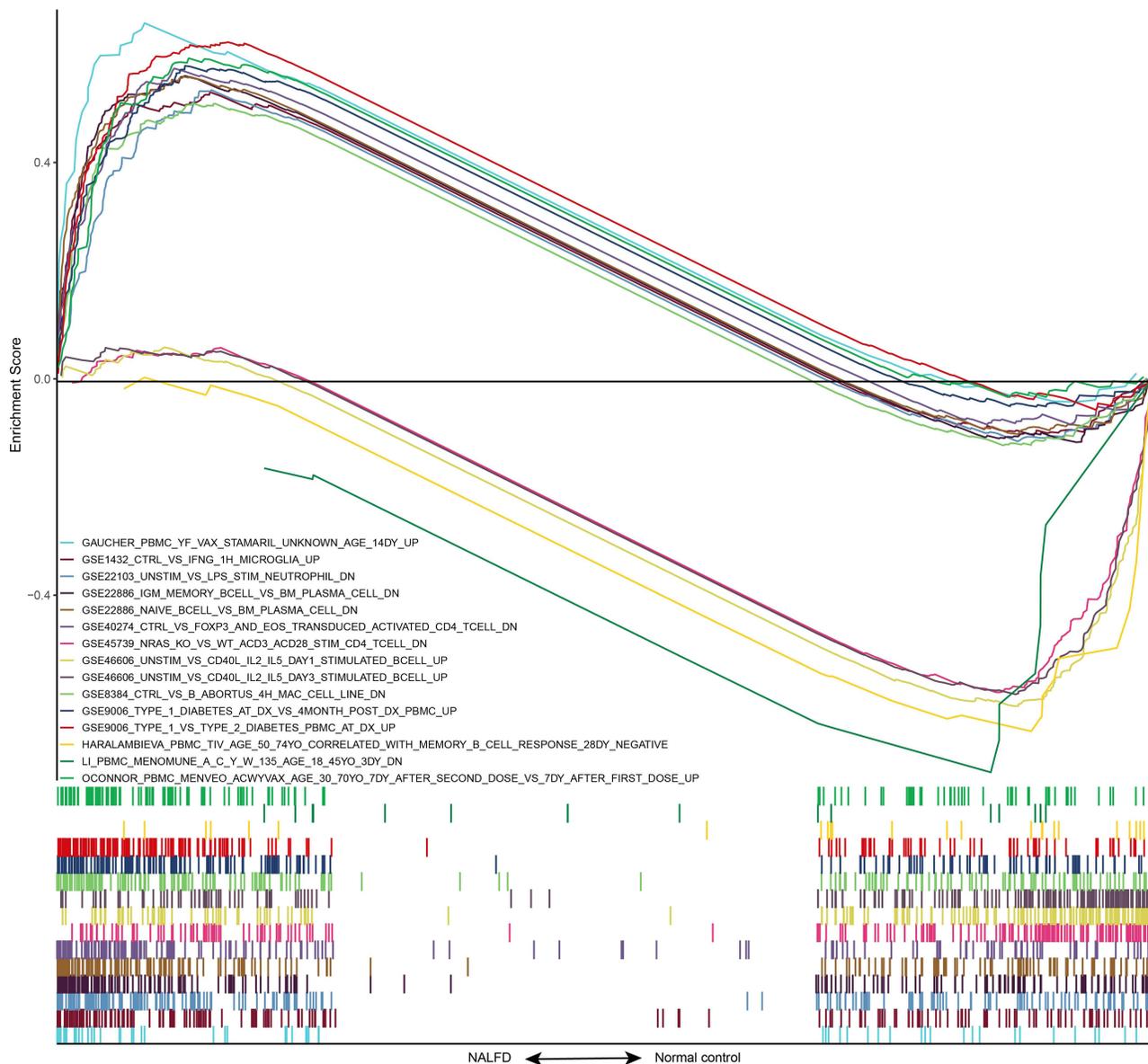
Figure 3 Enrichment plot for GSEA immunologic signature database.

axis activates immune function during infection. Mice lacking IL17RE are unable to fight infection.[38] This observation demonstrates the important role of IL17RE in activating immune function. However, uncontrolled activation can sometimes occur. IL17RE has been shown to exacerbate the course of autoimmune encephalitis,[39] and the IL-17C/IL17RE axis was shown to significantly promote renal tissue damage in a mouse model of crescentic nephritis.[40] To date, IL17-RE has been little studied in the liver. Some studies have reported that the IL-17C/IL17RE axis enhances T-cell function in autoimmune hepatitis and that high IL17RE expression is associated with poor prognosis in HCC.[41,42] Our data showed decreased expression levels of IL17RE in NAFLD. Similar to IL17RE, BACH2 is involved in T-cell regulation. BACH2 negatively regulates CD4+ T cells and can maintain CD4+ T cells in a naive state by suppressing effector memory-related genes.[43] Moreover, S100 calcium binding protein a was identified as a direct target gene of BACH2. In our study, the expression of both BACH2 and S100A9 was elevated in NAFLD, but the positive correlation between their
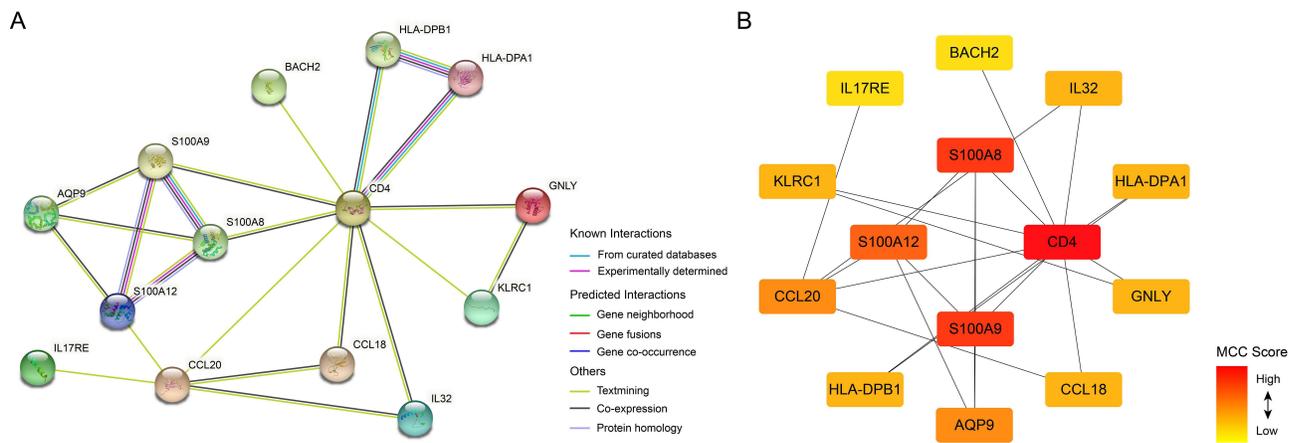
Figure 4 PPI network and MCC analysis. Construction of PPI network based on IRDEGs in STRING database and disconnected nodes were hided (**A**). The MCC scores of IRDEGs were analyzed using Cytohubba and displayed in Cytoscape software (**B**).
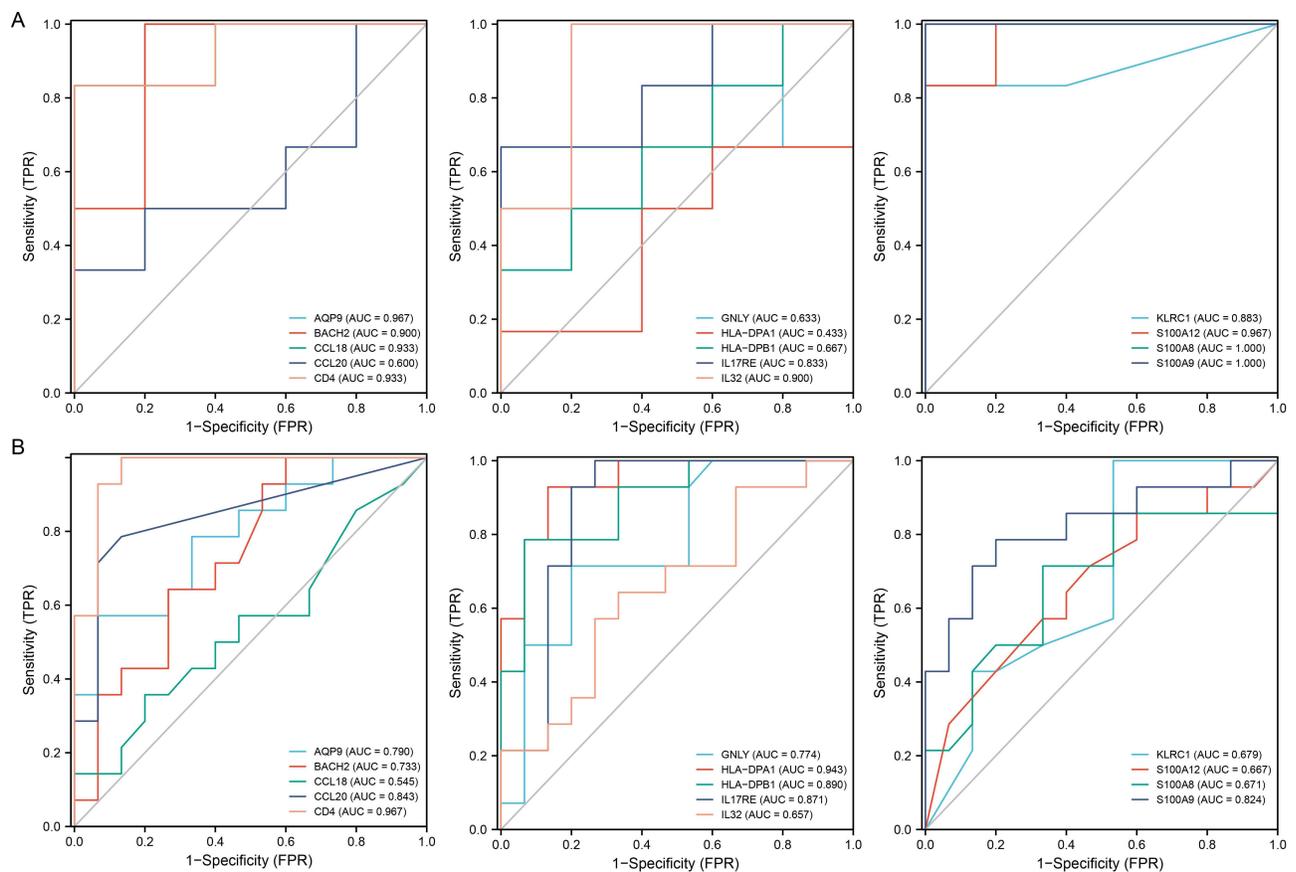

Figure 5 Diagnostic value of 14 IRDEGs in two datasets. The ROC curves of 14 IRDEGs in GSE160016 (**A**). The diagnostic value of 14 IRDEGs was validated using the data in GSE126848 (**B**).

expression was not statistically significant. In addition, some studies have demonstrated a low number of CD4+ T cells in NASH.[44] Considering the functions of IL17RE and BACH2, these results further demonstrate that immune function is suppressed in NAFLD.
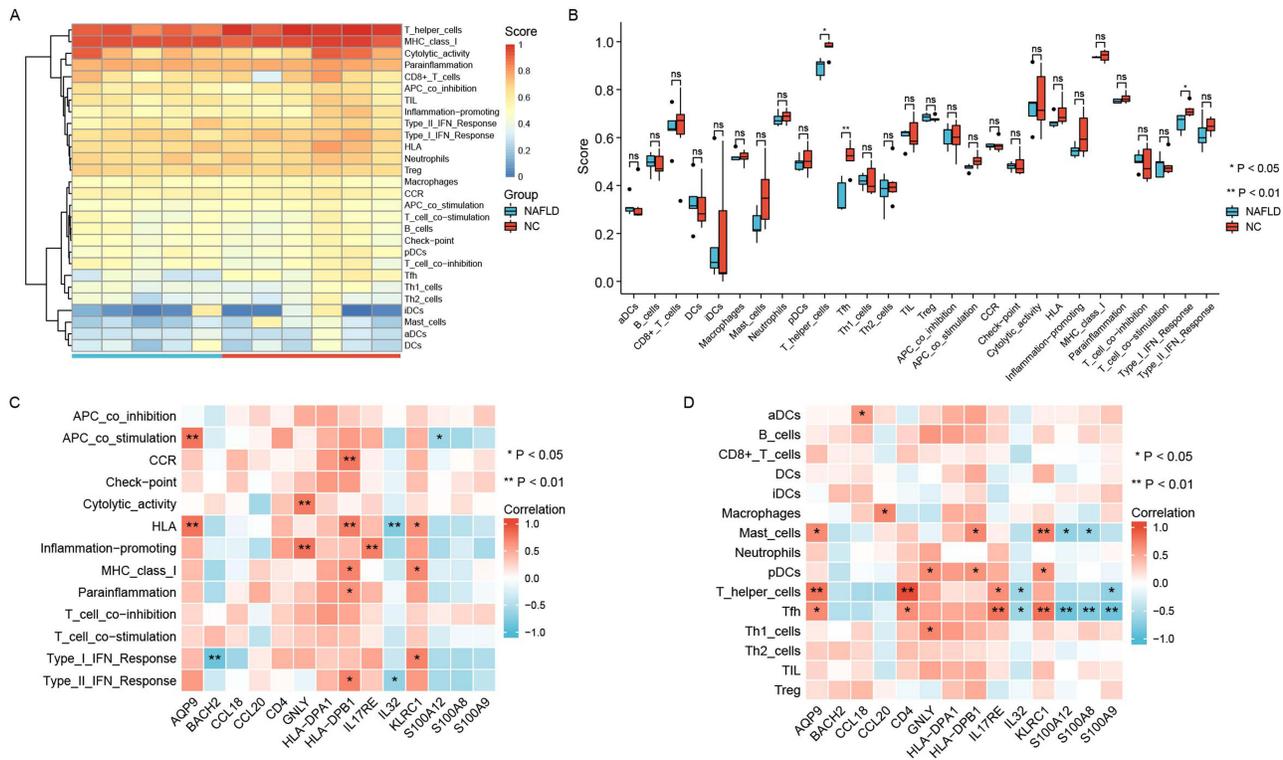
Figure 6 Correlation analysis between immune infiltration and IRDEGs. The heat map of immune infiltration levels (**A**). Box plot showed the level of identified immune cells and function between NAFLD and control samples (**B**). The correlation between IRDEGs and immune cells and function (**C** and **D**).
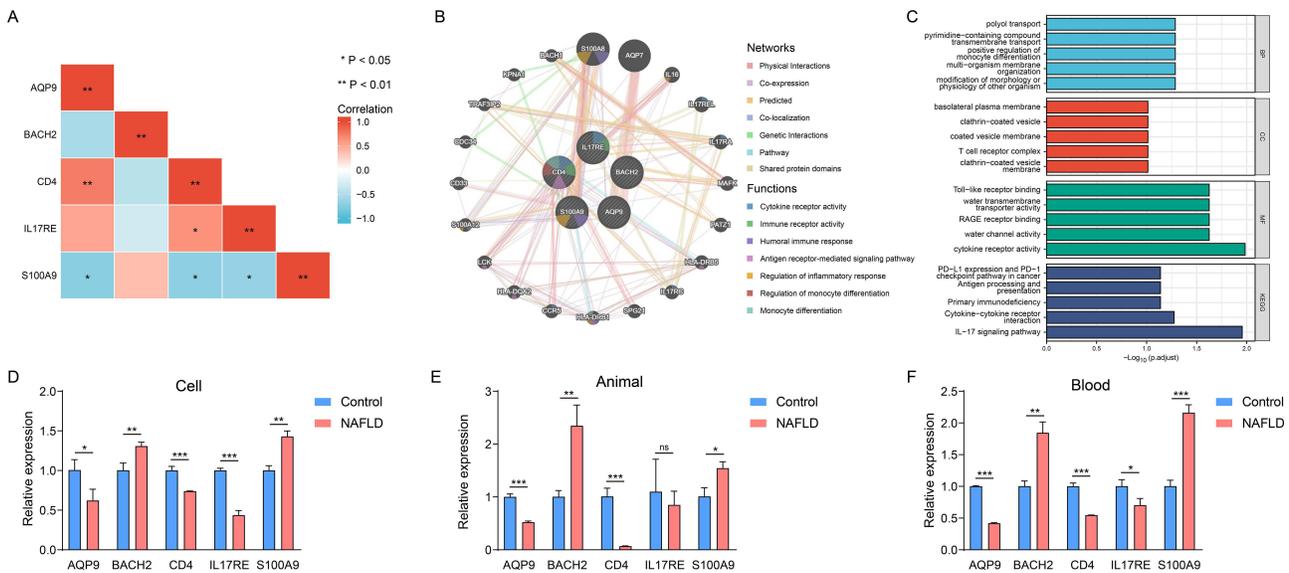

Figure 7 The function enrichment analysis and validation of hub IRDEGs. Heat map showed the correlation of hub IRDEGs expression (**A**). Hub IRDEGs and their co-expression genes were analyzed using GeneMANIA (**B**). GO and KEGG enrichment analysis of hub IRDEGs (**C**). Validation of hub IRDEGs expression in cell (**D**), animal model (**E**) and human blood (**F**) (*P < 0.05; **P < 0.01; ***P < 0.001).
Abbreviation: ns, not significant.

Although five immune-related genes with good diagnostic value in patients with NAFLD were identified in this study, some limitations remain. First, the findings need to be validated using tissue-based flow cytometry. Second, the associations between immune cells and related genes as well as disease severity require further estimation.
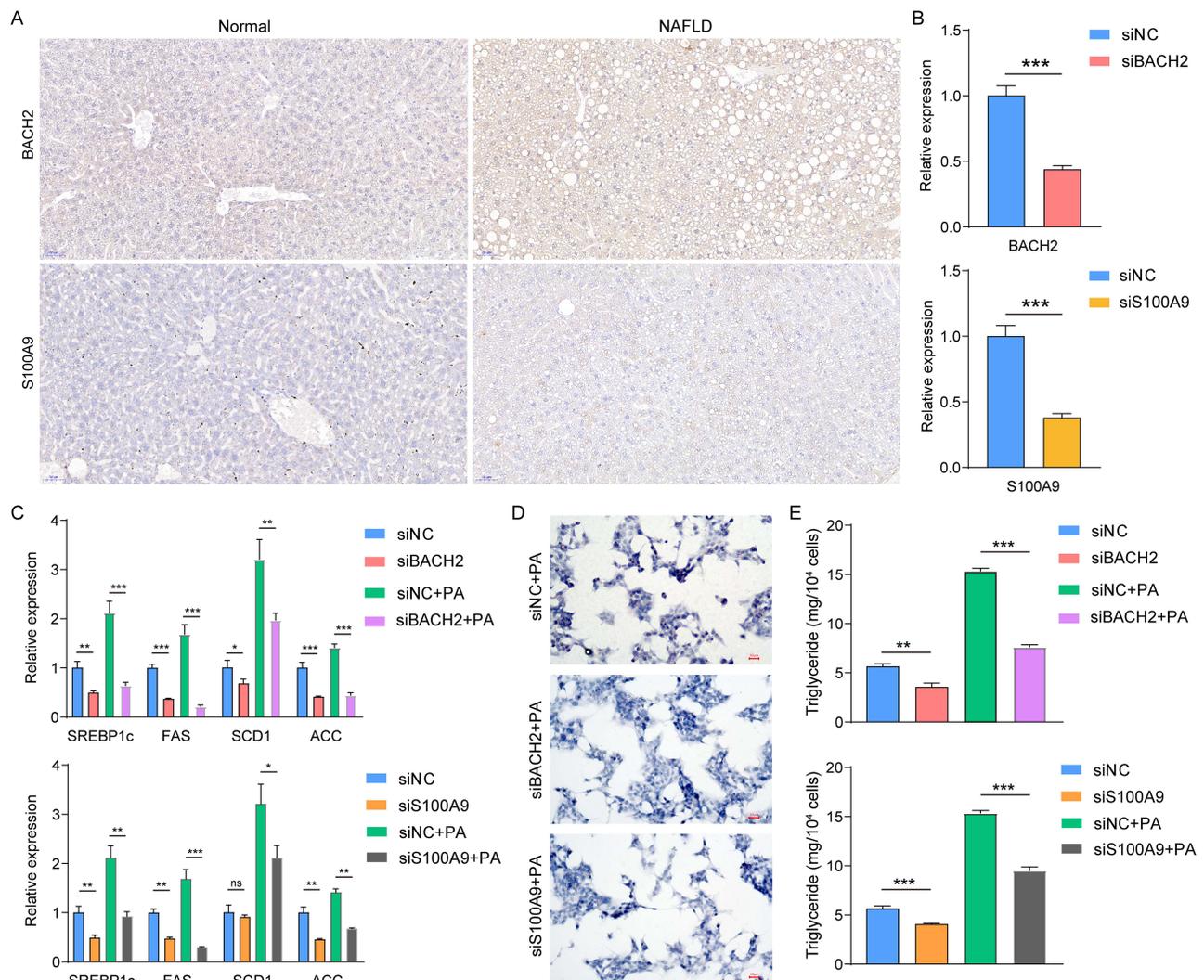
Figure 8 Detecting the role of BACH2 and S100A9 in NAFLD cells. Representative immunohistochemistry images of BACH2 and S100A9 in mice livers (scale bars, 50μm) (**A**). The knock-down of BAHC2 and S100A9 (***P < 0.001) (**B**). PCR to detect several maker genes of lipid accumulation after transfection (ns, not significant; *P < 0.05; **P < 0.01; ***P < 0.001) (**C**). Representative images of oil red O staining (scale bars, 50μm) (**D**). Triglyceride detection (**P < 0.01; ***P < 0.001) (**E**).

Conclusions

This study provided initial insight into immune infiltration in NAFLD and identified AQP9, CD4, IL17RE, BACH2 and S100A9 as ancillary diagnostic indicators of NAFLD. However, future studies that use flow cytometry to analyze larger samples and incorporate clinical information are necessary to validate these findings.

Availability of Supporting Data

The data generated during and/or analyzed during the current study are available from the corresponding author on reasonable request.

Ethical Approval and Consent to Participate

The study was conducted according to the guidelines of the Declaration of Helsinki and approved by the Biomedical Research Ethic Committee of Shandong Provincial Hospital (SWYX: NO. 2021-270; SWYX: NO. 2021-497).

Consent for Publication

All authors have read the final version of the manuscript and agreed to its publication.

Author Contributions

All authors made substantial contributions to conception and design, acquisition of data, or analysis and interpretation of data; took part in drafting the article or revising it critically for important intellectual content; agreed to submit to the current journal; gave final approval of the version to be published; and agree to be accountable for all aspects of the work.

Funding

Disclosure

The authors state that they have no conflicts of interest in this work.

References

1. Yip TC-F, Lee HW, Chan WK, et al. Asian perspective on NAFLD-associated HCC. *J Hepatol*. 2022;76(3):726–734. doi:10.1016/j.jhep.2021.09.024
2. Lazarus JV, Mark HE, Anstee QM, et al. Advancing the global public health agenda for NAFLD: a consensus statement. *Nat Rev Gastroenterol Hepatol*. 2022;19(1):60–78.
3. Li J, Zou B, Yeo YH, et al. Prevalence, incidence, and outcome of non-alcoholic fatty liver disease in Asia, 1999–2019: a systematic review and meta-analysis. *Lancet Gastroenterol Hepatol*. 2019;4(5):389–398. doi:10.1016/S2468-1253(19)30039-1
4. Chalasani N, Younossi Z, Lavine JE, et al. The diagnosis and management of non-alcoholic fatty liver disease: practice guideline by the American Association for the Study of Liver Diseases, American College of Gastroenterology, and the American Gastroenterological Association. *Hepatology*. 2012;55(6):2005–2023. doi:10.1002/hep.25762
5. Loomba R, Adams LA. The 20% rule of NASH progression: the natural history of advanced fibrosis and cirrhosis caused by NASH. *Hepatology*. 2019;70(6):1885–1888. doi:10.1002/hep.30946
6. Anstee QM, Reeves HL, Kotsiliti E, et al. From NASH to HCC: current concepts and future challenges. *Nat Rev Gastroenterol Hepatol*. 2019;16(7):411–428.
7. Nati M, Chung KJ, Chavakis T. The role of innate immune cells in nonalcoholic fatty liver disease. *J Innate Immun*. 2022;14(1):31–41. doi:10.1159/000518407
8. Meli R, Mattace Raso G, Calignano A. Role of innate immune response in non-alcoholic Fatty liver disease: metabolic complications and therapeutic tools. *Front Immunol*. 2014;5:177. doi:10.3389/fimmu.2014.00177
9. Arrese M, Cabrera D, Kalergis AM, et al. Innate immunity and inflammation in NAFLD/NASH. *Dig Dis Sci*. 2016;61(5):1294–1303. doi:10.1007/s10620-016-4049-x
10. Ma C, Kesarwala AH, Eggert T, et al. NAFLD causes selective CD4(+) T lymphocyte loss and promotes hepatocarcinogenesis. *Nature*. 2016;531(7593):253–257. doi:10.1038/nature16969
11. Hou J, Zhang J, Cui P, et al. TREM2 sustains macrophage-hepatocyte metabolic coordination in nonalcoholic fatty liver disease and sepsis. *J Clin Invest*. 2021;131(4). doi:10.1172/JCI135197
12. Ritchie ME, Phipson B, Wu D, et al. limma powers differential expression analyses for RNA-sequencing and microarray studies. *Nucleic Acids Res*. 2015;43(7):e47. doi:10.1093/nar/gkv007
13. Bhattacharya S, Dunn P, Thomas CG, et al. ImmPort, toward repurposing of open access immunological assay data for translational and clinical research. *Sci Data*. 2018;5:180015. doi:10.1038/sdata.2018.15
14. Bindea G, Mlecnik B, Tosolini M, et al. Spatiotemporal dynamics of intratumoral immune cells reveal the immune landscape in human cancer. *Immunity*. 2013;39(4):782–795. doi:10.1016/j.immuni.2013.10.003
15. Zhang X, Lan Y, Xu J, et al. CellMarker: a manually curated resource of cell markers in human and mouse. *Nucleic Acids Res*. 2019;47:D721–D728. doi:10.1093/nar/gky900
16. Subramanian A, Tamayo P, Mootha VK, et al. Gene set enrichment analysis: a knowledge-based approach for interpreting genome-wide expression profiles. *Proc Natl Acad Sci U S A*. 2005;102(43):15545–15550. doi:10.1073/pnas.0506580102
17. Li M, Xu C, Shi J, et al. Fatty acids promote fatty liver disease via the dysregulation of 3-mercaptopyruvate sulfurtransferase/hydrogen sulfide pathway. *Gut*. 2018;67(12):2169–2180. doi:10.1136/gutjnl-2017-313778
18. Park M, Yoo J-H, Lee Y-S, et al. Extract attenuates non-alcoholic fatty liver disease in free fatty acid-induced HepG2 hepatocytes and in high fat diet-fed mice. *Nutrients*. 2019;11(3):494. doi:10.3390/nu11030494
19. Jiang C, Xie C, Li F, et al. Intestinal farnesoid X receptor signaling promotes nonalcoholic fatty liver disease. *J Clin Invest*. 2015;125(1):386–402. doi:10.1172/JCI76738
20. Wang M, Li B, Qin F, et al. Obesity induced Ext1 reduction mediates the occurrence of NAFLD. *Biochem Biophys Res Commun*. 2022;589:123–130. doi:10.1016/j.bbrc.2021.12.017
21. Zhang L, Jiao G, Ren S, et al. Exosomes from bone marrow mesenchymal stem cells enhance fracture healing through the promotion of osteogenesis and angiogenesis in a rat model of nonunion. *Stem Cell Res Ther*. 2020;11(1):38. doi:10.1186/s13287-020-1562-9
22. You Y, Liu J, Zhang L, et al. WTAP-mediated m(6)A modification modulates bone marrow mesenchymal stem cells differentiation potential and osteoporosis. *Cell Death Dis*. 2023;14(1):33. doi:10.1038/s41419-023-05565-x
23. Zhao NQ, Li X-Y, Wang L, et al. Palmitate induces fat accumulation by activating C/EBPβ-mediated G0S2 expression in HepG2 cells. *World J Gastroenterol*. 2017;23(43):7705–7715. doi:10.3748/wjg.v23.i43.7705

24. Syn WK, Htun Oo Y, Pereira TA, et al. Accumulation of natural killer T cells in progressive nonalcoholic fatty liver disease. *Hepatology*. 2010;51 (6):1998–2007. doi:10.1002/hep.23599

25. Rau M, Schilling A-K, Meertens J, et al. Progression from nonalcoholic fatty liver to nonalcoholic steatohepatitis is marked by a higher frequency of Th17 Cells in the liver and an increased Th17/resting regulatory T cell ratio in peripheral blood and in the liver. *J Immunol*. 2016;196(1):97–105. doi:10.4049/jimmunol.1501175

26. du Plessis J, van Pelt J, Korf H, et al. Association of adipose tissue inflammation with histologic severity of nonalcoholic fatty liver disease. *Gastroenterology*. 2015;149(3):635–648.e14. doi:10.1053/j.gastro.2015.05.044

27. Wieser V, Adolph TE, Grander C, et al. Adipose type I interferon signalling protects against metabolic dysfunction. *Gut*. 2018;67(1):157–165. doi:10.1136/gutjnl-2016-313155

28. Rojek AM, Skowronski MT, Füchtbauer E-M, et al. Defective glycerol metabolism in aquaporin 9 (AQP9) knockout mice. *Proc Natl Acad Sci U S A*. 2007;104(9):3609–3614. doi:10.1073/pnas.0610894104

29. Gena P, Mastrodonato M, Portincasa P, et al. Liver glycerol permeability and aquaporin-9 are dysregulated in a murine model of non-alcoholic fatty liver disease. *PLoS One*. 2013;8(10):e78139. doi:10.1371/journal.pone.0078139

30. Rodríguez A, Gena P, Méndez-Giménez L, et al. Reduced hepatic aquaporin-9 and glycerol permeability are related to insulin resistance in non-alcoholic fatty liver disease. *Int J Obes*. 2014;38(9):1213–1220. doi:10.1038/ijo.2013.234

31. Wang C, Lv Z-L, Kang Y-J, et al. Aquaporin-9 downregulation prevents steatosis in oleic acid-induced non-alcoholic fatty liver disease cell models. *Int J Mol Med*. 2013;32(5):1159–1165. doi:10.3892/ijmm.2013.1502

32. Quoc QL, Choi Y, Thi Bich TC, et al. S100A9 in adult asthmatic patients: a biomarker for neutrophilic asthma. *Exp Mol Med*. 2021;53 (7):1170–1179. doi:10.1038/s12276-021-00652-5

33. Ding Z, Du F, Averitt V RG, et al. Targeting S100A9 reduces neutrophil recruitment, inflammation and lung damage in abdominal sepsis. *Int J Mol Sci*. 2021;22(23):12923. doi:10.3390/ijms222312923

34. Marinković G, Koenis DS, de Camp L, et al. S100A9 links inflammation and repair in myocardial infarction. *Circ Res*. 2020;127(5):664–676. doi:10.1161/CIRCRESAHA.120.315865

35. Agra RM, Fernández-Trasancos Á, Sierra J, et al. Differential association of S100A9, an inflammatory marker, and p53, a cell cycle marker, expression with epicardial adipocyte size in patients with cardiovascular disease. *Inflammation*. 2014;37(5):1504–1512. doi:10.1007/s10753-014-9876-3

36. Bouma G, Lam-Tse WK, Wierenga-Wolf AF, et al. Increased serum levels of MRP-8/14 in type 1 diabetes induce an increased expression of CD11b and an enhanced adhesion of circulating monocytes to fibronectin. *Diabetes*. 2004;53(8):1979–1986. doi:10.2337/diabetes.53.8.1979

37. Liu X, Wang Y, Ming Y, et al. S100A9: a potential biomarker for the progression of non-alcoholic fatty liver disease and the diagnosis of non-alcoholic steatohepatitis. *PLoS One*. 2015;10(5):e0127352. doi:10.1371/journal.pone.0127352

38. Nies JF, Panzer U. IL-17C/IL-17RE: emergence of a unique axis in T17 biology. *Front Immunol*. 2020;11:341. doi:10.3389/fimmu.2020.00341

39. Chang SH, Reynolds J, Pappu B, et al. Interleukin-17C promotes Th17 cell responses and autoimmune disease via interleukin-17 receptor E. *Immunity*. 2011;35(4):611–621. doi:10.1016/j.immuni.2011.09.010

40. Krohn S, Nies JF, Kapffer S, et al. IL-17C/IL-17 receptor E signaling in CD4 T cells promotes T17 cell-driven glomerular inflammation. *JASN*. 2018;29(4):1210–1222. doi:10.1681/ASN.2017090949

41. Huang J, Yuan Q, Zhu H, et al. IL-17C/IL-17RE augments T cell function in autoimmune hepatitis. *J Immunol*. 2017;198(2):669–680. doi:10.4049/jimmunol.1600977

42. Liao R, Sun J, Wu H, et al. High expression of IL-17 and IL-17RE associate with poor prognosis of hepatocellular carcinoma. *J Exp Clin Cancer Res*. 2013;32:3. doi:10.1186/1756-9966-32-3

43. Tsukumo S-I, Unno M, Muto A, et al. Bach2 maintains T cells in a naive state by suppressing effector memory-related genes. *Proc Natl Acad Sci U S A*. 2013;110(26):10735–10740. doi:10.1073/pnas.1306691110

44. Wang H, Zhang H, Wang Y, et al. Regulatory T-cell and neutrophil extracellular trap interaction contributes to carcinogenesis in non-alcoholic steatohepatitis. *J Hepatol*. 2021;75(6):1271–1283. doi:10.1016/j.jhep.2021.07.032